Electronic Supplementary Material (ESI) for ChemComm.

Supporting Information for manuscript

CO_2 conversion to phenyl isocyanates by uranium(VI) bis(imido) complexes

Leonor Maria,*[a,b] Nuno A. G. Bandeira,*[c] Joaquim Marçalo,[a,b]
Isabel C. Santos,[a] and John K. Gibson[d]

a. Centro de Ciências e Tecnologias Nucleares (C2TN), Instituto Superior Técnico, Universidade de Lisboa, 2695-066 Bobadela, Portugal. E-mail: leonorm@ctn.tecnico.ulisboa.pt
b. Centro de Química Estrutural (CQE), Instituto Superior Técnico, Universidade de Lisboa, 2695-066 Bobadela, Portugal.
c. BioISI and Centro de Química e Bioquiímica, Faculdade de Ciências, Universidade de Lisboa, 1749-016 Lisboa Portugal. E-mail: nuno.bandeira@ciencias.ulisboa.pt
d. Chemical Sciences Division, Lawrence Berkeley National Laboratory, Berkeley, CA 94720, USA.

Table of contents:

1. General considerations for synthesis

All reactions were performed under an inert atmosphere of nitrogen with the rigorous exclusion of oxygen and water (< 1 ppm), using standard Schlenk techniques or a nitrogen-filled glovebox. Solvents (tetrahydrofuran, toluene and *n*-hexane) were pre-dried using 4Å molecular sieves, distilled from Na/benzophenone under nitrogen, and deoxygenated immediately prior use. Benzene-d_6 and toluene-d_8 were vacuum distilled over sodium.

[U(κ^6-{(^{tBu2}ArO)$_2$Me$_2$-cyclam})I] (**1**) and [U(κ^4-{(^{tBu2}ArO)$_2$Me$_2$-cyclam})(NPh)$_2$] (**2**) were synthetized as previously described.[1] Azobenzene and 4-methylazobenzene were purchased from Aldrich, sublimed and dried in vacuum, respectively, prior to use. ^{1}H and ^{13}C NMR spectra were recorded in Bruker AVANCE 300 or 400 MHz spectrometers. ^{1}H and ^{13}C chemical shifts were referenced to external SiMe$_4$ using the residual proton or carbon of the solvents as internal standards. IR spectra were recorded as Nujol mulls between KBr round cell windows on a Bruker Tensor 27 FTIR spectrophotometer. CHN elemental analyses were performed using a CE Instruments EA1110 automatic analyser.

High resolution ESI(+) mass spectra were obtained on a QqTOF Impact II^{TM} mass spectrometer (Bruker Daltonics, Bremen, Germany) operating in the high resolution mode. The TOF analyser was calibrated in the *m/z* range 500-1500 using an internal calibration standard (Tune mix solution) which is supplied by Agilent. The full scan mass spectrum was acquired over a range of 500-1350 *m/z,* at a spectra rate of 1 Hz. Data was processed using Data Analysis 4.2 software. The uranium complex solution (ca. 1X10^{-5} M; the compound was first dissolved in thf and then diluted in acetonitrile) was prepared in the glove-box and maintained under nitrogen until injection into the spectrometer.

2. Synthesis

2.1. Reaction of 1 with 4-methylazobenzene. Isolation of [U(κ^4-{(^{tBu2}ArO)$_2$Me$_2$-cyclam})(NPh)(NPh^{Me})] (3).

To a stirring violet toluene (10 mL) solution of **1** (185 mg, 0.180 mmol, 2 equiv.) was added a 0.5 mL toluene solution of 4-methylazobenzene (18 mg, 0.090 mmol, 1 equiv.). Upon addition, the solution color changed to brown and the reaction mixture was vigorously stirred during 2h at room temperature. A yellow-green solid precipitated and was separated from the resulting brown-solution by centrifugation. The supernatant was taken to dryness and extracted with 8 mL of a mixture of *n*-hexane / thf (99/1). Then the solution was concentrated and centrifuged to isolate [U(κ^4-{(^{tBu2}ArO)$_2$Me$_2$-cyclam})(NPh)(NPh^{Me})] (**3**) as a brown crystalline solid (76 mg, 0.069 mmol, 77 %). Brown crystals of **3** suitable for single crystal X-ray diffraction analysis were grown by slow evaporation of n-hexane/thf solution of **3**. The yellow-green solid, identified as [U(κ^6-{(^{tBu2}Ar)$_2$Me-cyclam})I][I][1] by ^{1}H NMR, was isolated in 82 % yield (85 mg, 0.074 mmol) after being washed with toluene, *n*-hexane and vacuum-dried.

^{1}H NMR (300 MHz, benzene-*d*$_6$, 23ºC): δ = 7.94 (d, $^4J_{HH}$ = 2.4 Hz, 1H, Ar-H), 7.92 (d, $^4J_{HH}$ = 2.4 Hz, 1H, Ar-H), 7.69 (d, $^4J_{HH}$ = 2.7 Hz, 1H, Ar-H), 7.68 (d, $^4J_{HH}$ = 2.6 Hz, 1H, Ar-H), 6.98 (t, J$_{HH}$ = 7.8 Hz, *m*-Ar (imido), 2H), 6.81 (d, *J* = 8.1 Hz, 2H), 6.54 (d, J_{HH} = 12.1 Hz, NC*H*$_2$Ar, 1H), 6.52 (d, J_{HH} = 12.0 Hz, NC*H*$_2$Ar, 1H), 5.58 (m, C*H*$_2$, 2H), 5.48 (t, J_{HH} = 7.4 Hz, *p*-Ar (imido), 1H), 5.05 (d, J_{HH} = 7.4 Hz, *o*-Ar (imido), 2H), 4.97 ((d, J_{HH} = 8.2 Hz, *o*-Ar (imido) 2H), 3.88 (d, J_{HH} = 13.0 Hz, C*H*$_2$, 2H), 3.81 (d, J_{HH} = 12.3 Hz, NC*H*$_2$Ar, 2H), 3.24 (m, C*H*$_2$, 2H), 3.09 (m, C*H*$_2$, 2H), 2.78 (t, C*H*$_2$, 2H), 2.60 (br, CH$_2$C*H*$_2$CH$_2$, 2H), 2.57 (s, Ar-CH$_3$ (imido), 3H) 2.06 (s, NC*H*$_3$, 6H), 1.93 (br, C*H*$_2$, 2H), 1.87 (s, C(C*H*$_3$)$_3$, 9H), 1.85 (s, C(C*H*$_3$)$_3$), 1.62 (s, C(C*H*$_3$)$_3$, 9H), 1.60 (s, C(C*H*$_3$)$_3$ + CH2C*H*$_2$CH$_2$, 9H+2H), 1.56 (br,CH$_2$, 2H), 1.42 (br, C*H*$_2$, 2H).

^{13}C{^{1}H} NMR (75.4 MHz, benzene-*d*$_6$, 23°C): δ = 166.56, 166.50 (ArC-O), 153.90, 153.27 (*ipso*-Ar (imido)), 141.37 (Ar), 141.35 (Ar), 139.40 (Ar), 139.39 (Ar), 136.39 (Ar*C*-CH$_3$(imido)), 129.09 (*o*-Ar (imido)), 129.03 (*o*-Ar (imido)), 126.92 (Ar*C*-H), 126.73 (Ar), 126.68 (Ar), 126.61 (*p*-Ar(imido), 124.70 (*m*-Ar(imido)), 124.68, (*m*-Ar(imido)), 124.01 (Ar*C*-H), 123.97 ((Ar*C*-H), 63.61, 63.58 (Ar*C*H$_2$N), 59.07, 59.03 (*C*H$_2$), 56.78 (*C*H$_2$), 56.07, 56.03 (*C*H$_2$), 55.93, 55.89 (*C*H$_2$), 43.31, 43.30 (N*C*H3), 36.08, 36.06 (*C*(CH$_3$)$_3$), 34.30, 34.28 (*C*(CH$_3$)$_3$), 32.71, (C(*C*H$_3$)$_3$), 31.23, 32.17 (C(*C*H$_3$)$_3$), 25.38, 25.31 (CH$_2$*C*H$_2$CH$_2$), 18.93 (CH$_3$-imido).

Analysis for $C_{55}H_{82}N_6O_2U$: Calcd. C, 60.20 H, 7.53; N, 7.66; Found: C, 60.01; H, 7.45; N, 7.52.

IR (KBr plates, Nujol mull, ν/cm^{-1}): 1600 (w), 1582 (w), 1377 (s), 1293 (m), 1260 (s), 1240 (s), 1166 (w), 1129 (w), 1063 (w), 934 (m), 834 (m), 813 (m), 751 (m), 532 (w), 442 (w).

2.2. Reaction of 2 and 3 with excess of CO$_2$.

2.2.1. NMR tube scale reaction. 28 mg (0.025 mmol) of [U(κ^4-{(^{tBu2}ArO)$_2$Me$_2$-cyclam})(NPh)$_2$] (**2**) were dissolved in 0.5 mL of benzene-*d*$_6$. The solution contained in a J-Young NMR tube was freeze-vacuum-thawed (3x) and then an excess of CO$_2$ (ca. 30 equiv.) was condensed into the frozen brown solution. The solution was allowed to warm to room temperature and slowly changed from brown to dark red cherry. The reaction was monitored using ^{1}H NMR spectroscopy. The complete conversion of **2** to [U(κ^4-{(^{tBu2}ArO)$_2$Me$_2$-cyclam})(NPh)(O)] (**4**) and PhNCO was observed after 7 hours. A corresponding procedure was used to examine the reactivity of [U(κ^4-{(^{tBu2}ArO)$_2$Me$_2$-cyclam})(NPh)(NPh^{Me})] (**3**) with CO$_2$.

2.2.2. Synthesis of [U(κ^4-{(^{tBu2}ArO)$_2$Me$_2$-cyclam})(NPh)(O)] (4)

An ampoule was charged with [U(κ^4-{(^{tBu2}ArO)$_2$Me$_2$-cyclam})(NPh)$_2$] (**2**) (100 mg, 0.092 mmol) dissolved in 4.5 mL of toluene. The solution was freeze-vacuum-thawed (3x) and then an excess of CO_2 (ca. 24 equiv.) was condensed into the frozen solution. The solution was allowed to warm up to room temperature and stirred during 25 h, with the color slowly changing from brown to dark red cherry. Then all volatiles were removed under reduced pressure and the resulting solid was extracted with *n*-hexane and concentrated to afford a dark red cherry microcrystalline solid in 72 % yield (67 mg, 0.066 mmol). Crystals of **4** suitable for X-ray diffraction were grown by slow evaporation of a hexane solution of **4**. The amount of crystals isolated were not enough for elemental analysis.

When complex **4** is isolated, the solid shows a small contamination of a product (observed by NMR spectroscopy), which presumably results from the dimerization of phenyl isocyanate.[2] Complex **4** shows high solubility in toluene, benzene, thf, *n*-hexane, diethyl ether and dichloromethane and the side product seems to have similar solubility. Several attempts of recrystallization with different solvents were done in order to isolate a pure sample; however, the elemental analyses were always of reduced quality. The best analysis was the following: Calcd. for $C_{48}H_{75}N_3O_3U$: C, 57.18 H, 7.50; N, 6.95; Found for solid isolated from slow evaporation of a diethyl ether solution of **4**: C, 57.31; H, 8.64; N, 5.97.

^{1}H NMR (400 MHz, C_6D_6) δ 7.93 (d, $^4J_{HH}$ = 2.4 Hz, 1H, Ar-H), 7.83 (d, $^4J_{HH}$ = 2.4 Hz, 1H, Ar-H), 7.55 (d, $^4J_{HH}$ = 2.1 Hz, 1H, Ar-H), 7.51 (d, $^4J_{HH}$ = 2.5 Hz, 1H, Ar-H), 6.93 (t, J_{HH} = 7.7 Hz, 2H, *m*-imido), 6.08 (d, J_{HH} = 12.1 Hz, 1H, NCH_2Ar), 6.01 (d, J_{HH} = 12.3 Hz, 1H, NCH_2Ar), 5.76 (t, J_{HH} = 7.4 Hz, 1H, *p*-imido), 5.41 (t, 1H, CH_2), 5.32 (t, 1H, CH_2), 5.24 (d, J_{HH} = 7.7 Hz, 2H, *o*-imido), 3.82 (d, 1H, CH_2), 3.61-3.44 (m, 3H, CH_2+NCH_2Ar), 3.07 (t,1H, CH_2), 3.14-2.73 (m, 4H, CH_2), 2.63-2.44 (m, 2H+1H, $CH_2CH_2CH_2$+CH_2), 2.06 (s, 9H, $C(CH_3)_3$), 2.01 (s, 3H, NCH_3), 1.99 (s, 3H, NCH_3), 1.92-1.85 (m, 2H, CH_2), 1.82 (s, 9H, $C(CH_3)_3$), 1.76 (br, 1H, CH_2), 1.58 (s, 9H+1H, $C(CH_3)_3$), 1.56 (s, 9H, $C(CH_3)_3$), 1.59-1.55 (br, 2H, $CH_2CH_2CH_2$+CH_2), 1.50-1.45 (m, 2H, CH_2+$CH_2CH_2CH_2$), 1.22-1.15 (1H, CH_2).

^{13}C{^{1}H} NMR (75 MHz, C_6D_6) δ 166.74 (ArC-O), 166.56 (ArC-O), 153.59 (*ipso*-Ar (imido), 141.39 (Ar), 141.03 (Ar), 139.56 (Ar), 138.97 (Ar), 127.90 (*o*-Ar(imido)), 126.86 (ArC-H), 126.48 (ArC-H), 126.47 (Ar), 126.32 (*p*-Ar(imido)), 125.66 (*m*-Ar(imido)), 124.21 (ArC-H), 124.11 (ArC-H), 63.94 (NCH_2Ar), 63.31 (NCH_2Ar), 58.61 (CH_2), 58.48 (CH_2), 56.57 (CH_2), 56.39 (CH_2), 55.97 (CH_2), 55.78 (CH_2), 55.51 (CH_2), 54.64 (CH_2), 43.16 (NCH_3), 36.11 ($C(CH_3)_3$), 35.95($C(CH_3)_3$), 34.27 ($C(CH_3)_3$), 34.24 ($C(CH_3)_3$), 32.65 ($C(CH_3)_3$), 32.60 ($C(CH_3)_3$), 31.54 ($C(CH_3)_3$), 31.24 ($C(CH_3)_3$), 25.75 ($CH_2CH_2CH_2$), 24.94 ($CH_2CH_2CH_2$).

IR (KBr plates, Nujol mull, ν/cm^{-1}): 1598 (w), 1560 (w), 1377 (s), 1302 (w), 1262 (m), 1239 (s), 1202 (w), 1166 (w), 1131 (w), 1065 (w), 1014 (w), 945 (m), 913 (w), 879 (w), 833 (m), 807 (w), 752 (m), 728 (m), 692 (w), 532 (w), 441 (w).

ESI(+)-HRMS: *m/z* calcd. for $[M+H]^+$: 1008.6450; found: 1008.6439.

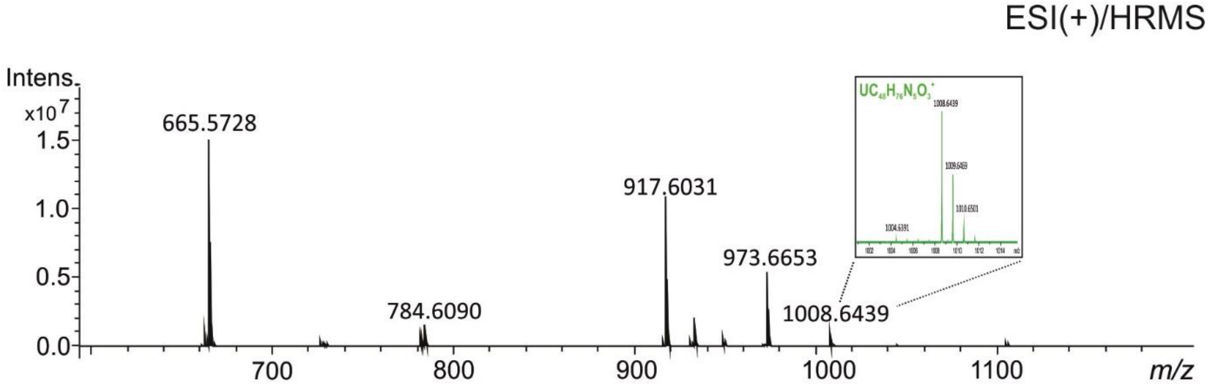

Figure S1. ESI(+)-HRMS of [UL(NPh)(O)] (**4**) in acetonitrile (with a small amount of thf). Complex **4** is very sensitive to water and it hydrolyses rapidly during the experiment, leading to $[LH_2 + H]^+$ at *m/z* 665.5728. The peaks at *m/z* 917.6031 ($[ULOH]^+$) and *m/z* 973.6653 ($[ULOBu]^+$) result from a very small contamination with the complex [ULI]I formed during the synthesis of $[UL(NPh)_2]$, which, as a cationic compound, is much easier to be detected by ESI(+)-MS.

3. X-ray crystallography

Crystallographic and experimental details of data collection and crystal structure determinations for the compounds are given in Table S1. Suitable crystals of compounds **3** and **4** were selected and coated in FOMBLIN oil under an inert atmosphere. Crystals were then mounted on a loop and the data were collected using graphite-monochromated Mo Kα (α=0.71073 Å) on a Bruker AXS-KAPPA APEX II area detector and data were collected at 150 K. Cell parameters were retrieved using Bruker SMART and refined using Bruker SAINT on all observed reflections.[3] Absorption corrections were applied using SADABS.[4] The structures were solved by direct methods using SHELXS[5] and refined using full-matrix least squares refinement against F^2 using SHELXL.[6] In the former case, all programs are included in the package of programs WINGX-version 2014.[7] All non-hydrogen atoms were refined anisotropically, unless it was mentioned in the cif files of the structures, and all hydrogen atoms were placed in idealized positions and allowed to refine riding on the parent carbon atom.

Table S1. Selected Crystal Data and Data Collection Parameters for **3** and **4**

	3	**4**
Empirical formula	$C_{55}H_{82}N_6O_2U$	$C_{48}H_{75}N_5O_3U$
Crystal size (mm)	0.18 x 0.08 x 0.04	0.14 x 0.08 x 0.06
Formula weight	1097.30	1008.16
Cryst. System	Triclinic	Monoclinic
Space group	P-1	P21/n
a [Å]	13.3531(7)	15.5464(6)
b[Å]	13.9911(6)	13.2994(5)
c [Å]	16.8717(9)	23.2853(8)
α [°]	103.238(3)	90
β [°]	108.535(2)	103.1120(10)
γ [°]	108.528(3)	90
V[Å^3]	2635.8(2)	4688.9(3)
Z	2	4
Calculated density (mg/m^{-3})	1.383	1.428
μ (mm^{-1})	3.124	3.506
T_{min}/T_{max}	0.6033 / 0.8852	0.6396 / 0.8172
F(000)	1124	2056
θ_{max} (º)	25.03	25.68
Reflections collected	12820	37084
Unique refl. (R_{int})	8104 (0.0436)	8873 (0.0658)
R_1[I>2σ(I)]	0.0577	0.0338
wR2 (all data)	0.1496	0.0739
Parameters	580	527
GOF on F^2	0.989	1.005
Largest diff. peak , hole/e Å^{-3}	3.146, -1.971	1.088, -0.816

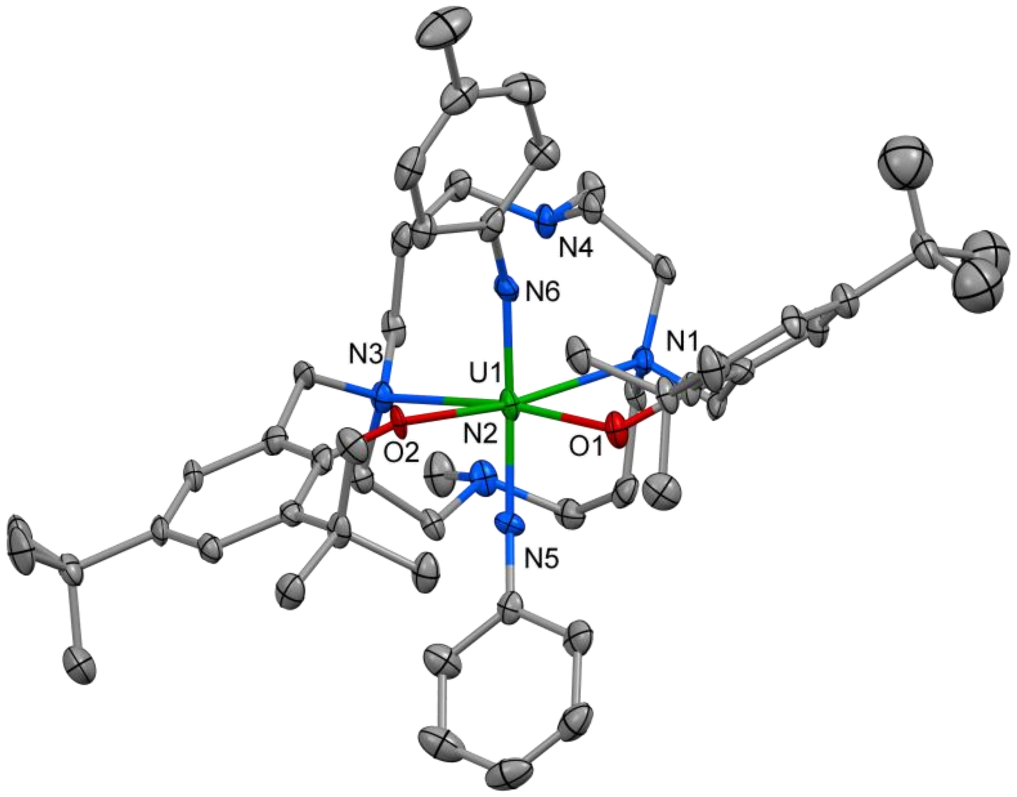

Figure S2. Molecular structure of $[U(\kappa^4\text{-}\{(^{tBu2}ArO)_2Me_2\text{-cyclam}\})(=NPh)(=Ntol)]$ (**3**)

Table S2. Selected bond distances (Å) and angles (°) of complexes $[U(\kappa^4\text{-}\{(^{tBu2}ArO)_2Me_2\text{-cyclam}\})(=NPh)(=Ntol)]$ (**3**) and $[U(\kappa^4\text{-}\{(^{tBu2}ArO)_2Me_2\text{-cyclam}\})(=NPh)(O)]$ (**4**).

	3	4
U-N$_{imido}$	1.909(6), 1.911(7)	1.879(3)
U-O$_{oxo}$	-	1.787(3)
U-O$_{Ar}$	2.170(6), 2.163(5)	2.168(3), 2.191(3)
U-N$_{cyclam}$	2.738(6), 2.713(8)	2.779(3), 2.768(3)
N$_{imido}$-U-N$_{imido}$	**173.7(3)**	-
U-N-C$_{ipso}$	152.9(6), 152.1(6)	156.9(3)
O-U-N$_{imido}$	-	**176.37(14)**
O$_{Ar}$-U-O$_{Ar}$	105.1(2)	106.96(10)
N$_{cyclam}$-U-N$_{cyclam}$	99.4(2)	99.3(1)
O$_{Ar}$-U-N$_{cyclam}$(trans)	170.8(2), 172.35(19)	170.59(10), 170.17(10)

4. NMR Data

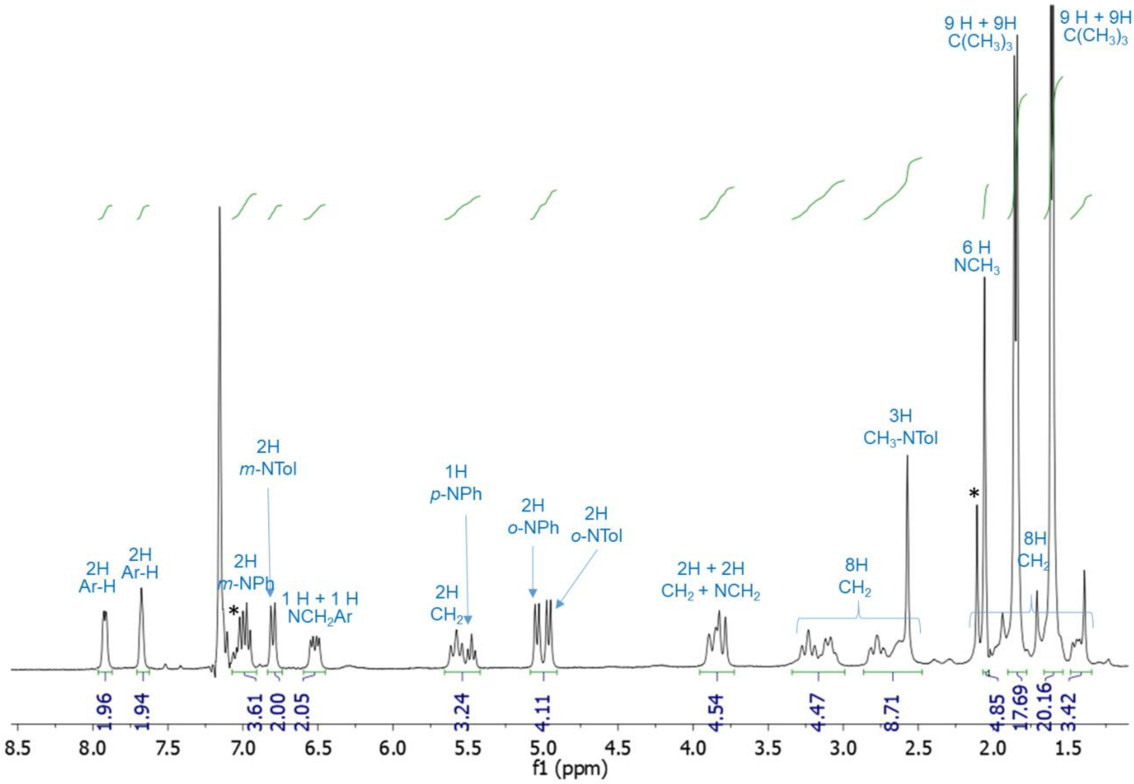

Figure S3. ^{1}H NMR of [U(κ^4-{(^{tBu2}ArO)$_2$Me$_2$-cyclam})(NPh)(NTol)] (**3**) in benzene-d_6 at 25 °C (*residual toluene). The CH$_2$ proton assignment as based on the ^{1}H-^{13}C HSQC and ^{1}H-^{1}H COSY.

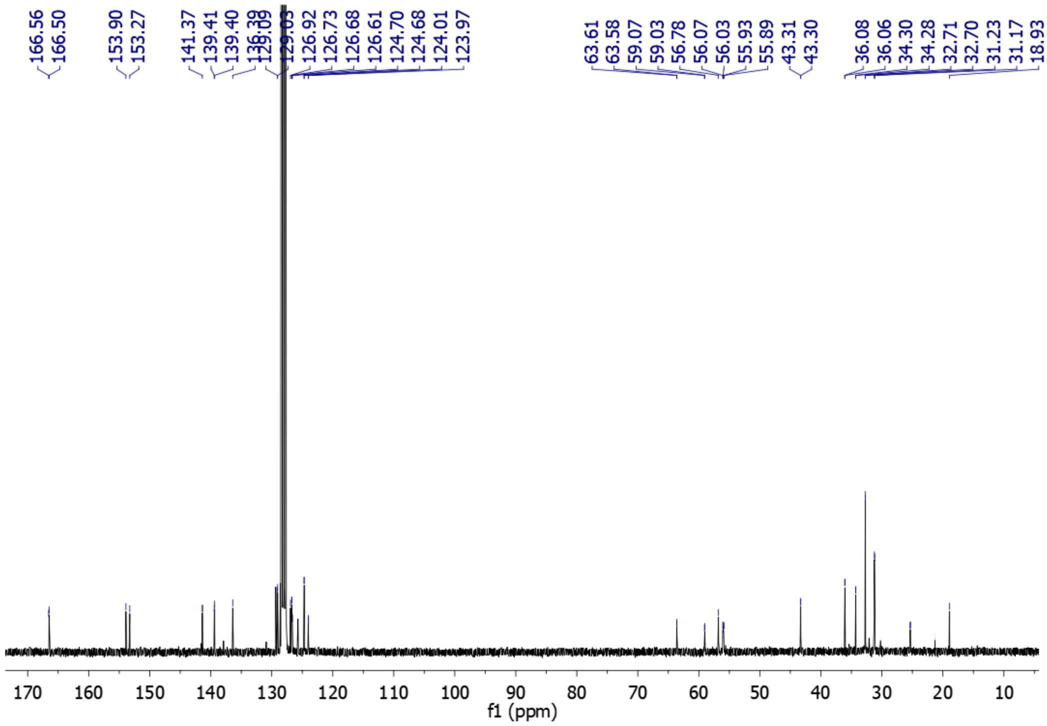

Figure S4. ^{13}C NMR of [U(κ^4-{(^{tBu2}ArO)$_2$Me$_2$-cyclam})(NPh)(NTol)] (**3**) in benzene-d_6 at 25 °C .

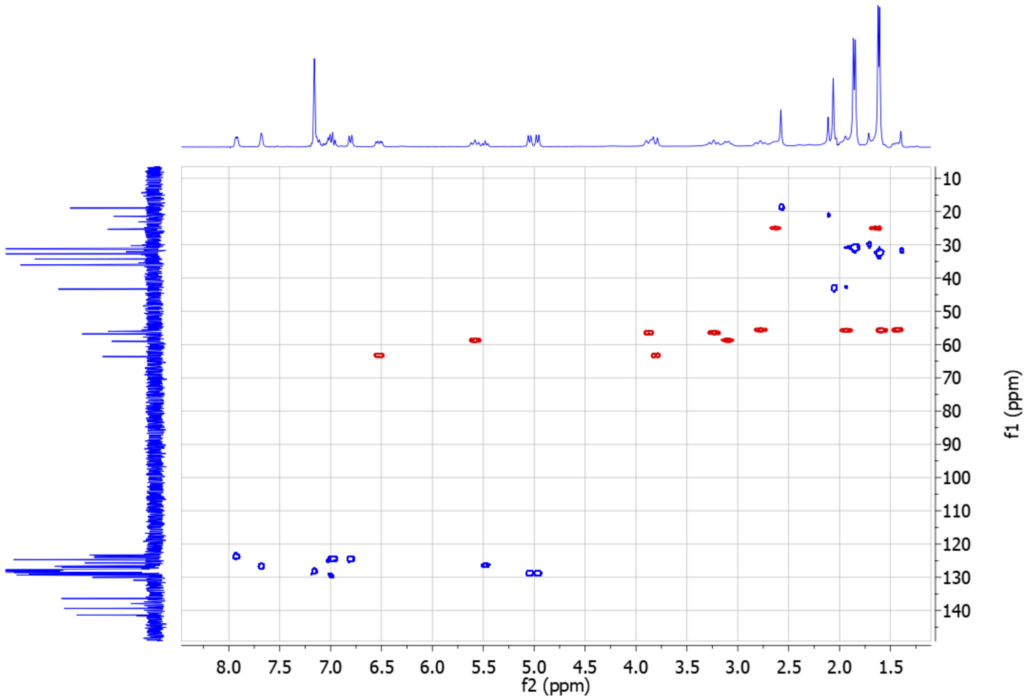

Figure S5. ^{1}H - ^{13}C multiplicity-edited HSQC of [U(κ^4-{(^{tBu2}ArO)$_2$Me$_2$-cyclam})(=NPh)(=NTol)] (**3**) in benzene-*d*$_6$ at 25 °C (CH_2 correlations in red; CH_3/CH correlations in blue).

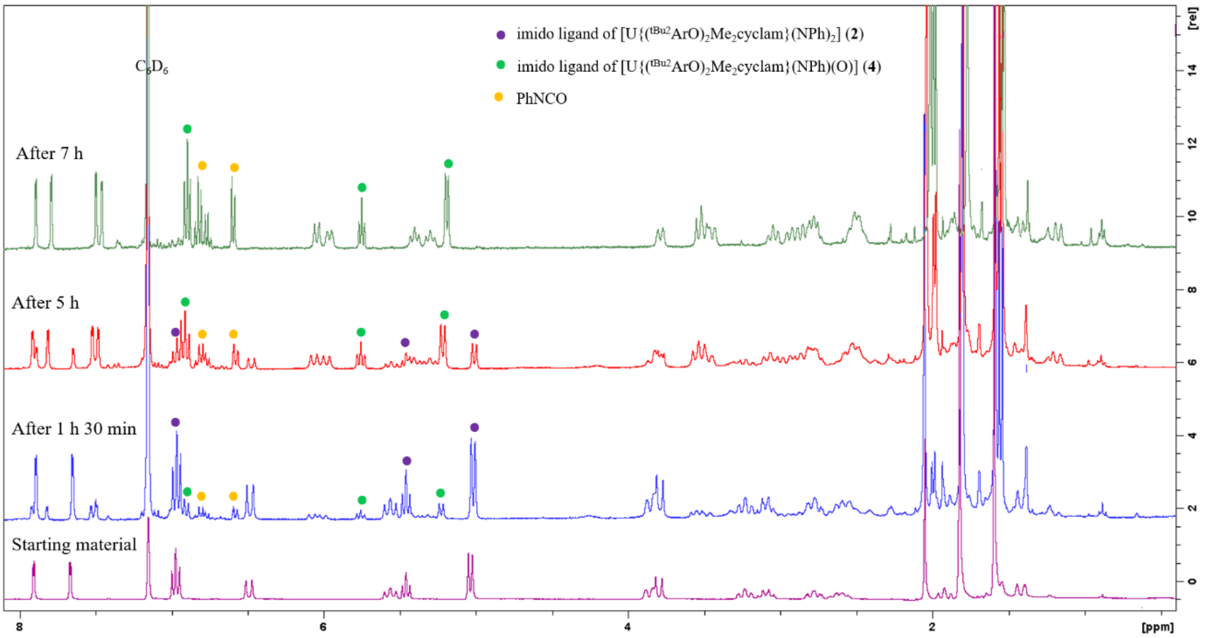

Figure S6. Reaction evolution over time of the ^{1}H NMR spectrum of the reaction of [U(κ^4-{(^{tBu2}ArO)$_2$Me$_2$-cyclam})(NPh)$_2$] (**2**) with excess of CO_2 in benzene-*d*$_6$.

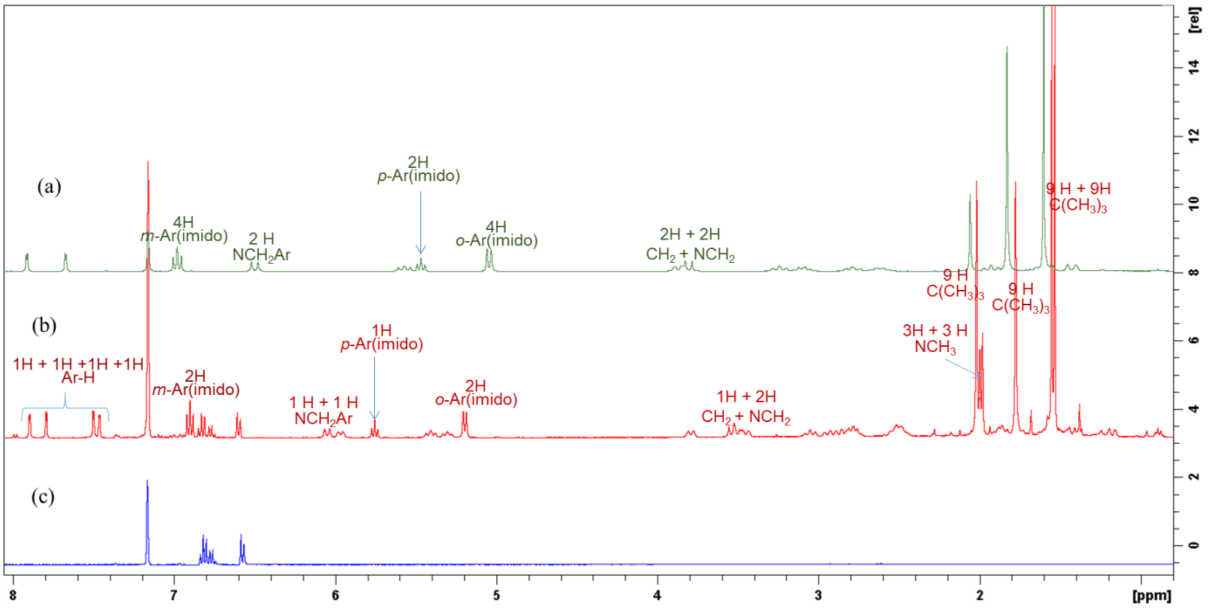

Figure S7. ^{1}H NMR spectrum (benzene-d_6, 25 °C) of (a) [U(κ^4-{(^{tBu2}ArO)$_2$Me$_2$-cyclam})(NPh)$_2$] (**2**); (b) NMR tube scale reaction of [U(κ^4-{(^{tBu2}ArO)$_2$Me$_2$-cyclam})(NPh)$_2$] (**2**) with excess of CO_2 (ca. 30 equiv.) after 7 h; (c) free phenyl isocyanate.

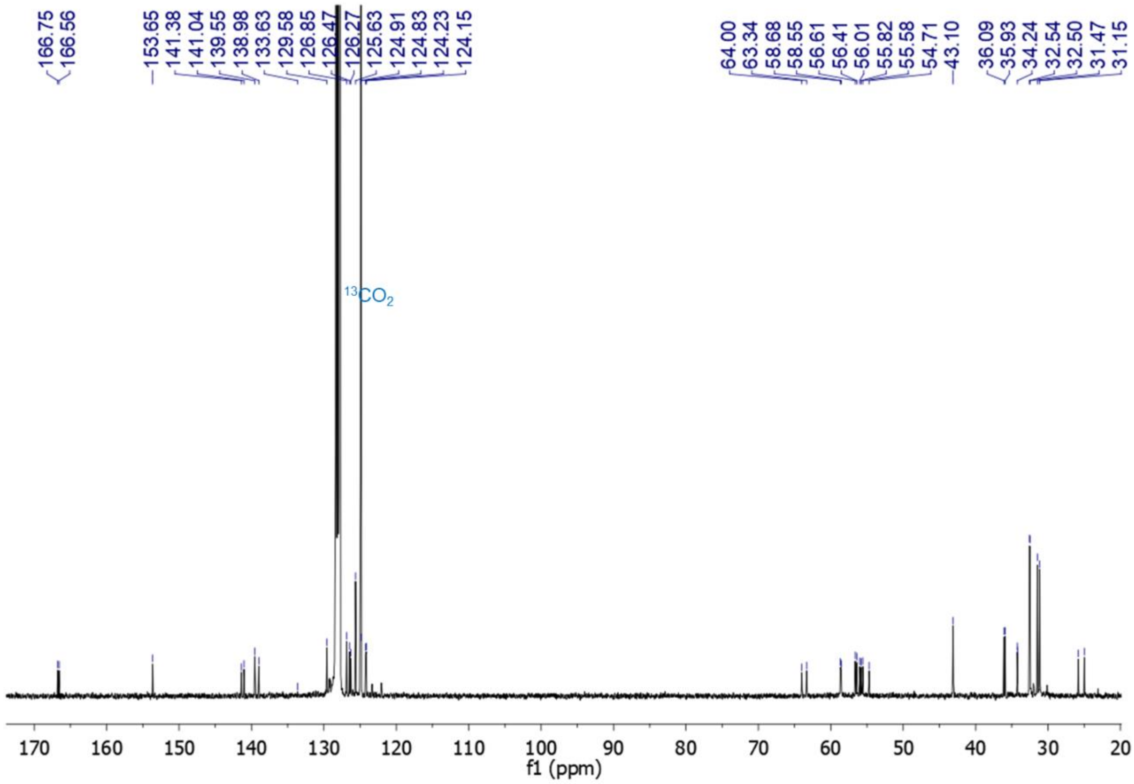

Figure S8. ^{13}C{H} NMR spectrum (benzene-d_6, 25 °C) of the NMR tube scale reaction of [U(κ^4-{(^{tBu2}ArO)$_2$Me$_2$-cyclam})(NPh)$_2$] (**2**) with CO_2 (ca. 30 equiv.).

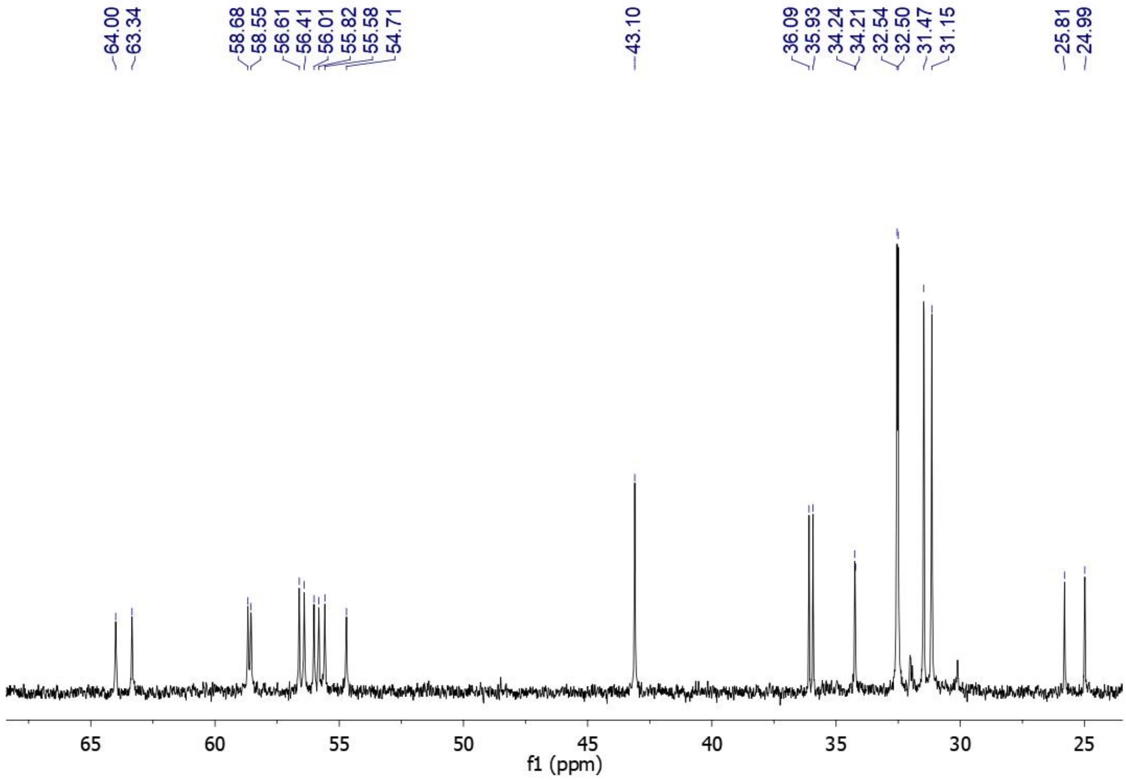

Figure S9. $^{13}C\{H\}$ NMR spectrum (benzene-d_6, 25 °C) (70- 24 ppm) of the NMR tube scale reaction of $[U(\kappa^4\text{-}\{(^{tBu2}ArO)_2Me_2\text{-cyclam}\})(NPh)_2]$ (**2**) with of CO_2 (ca. 30 equiv.).

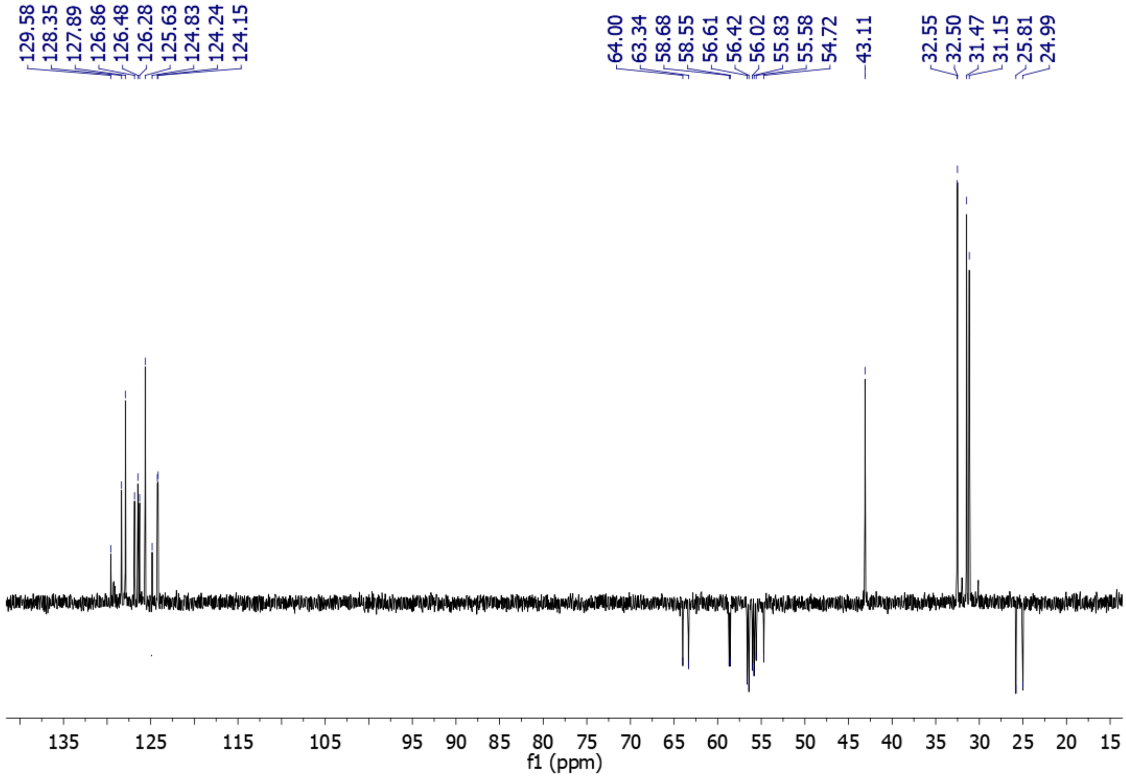

Figure S10. ^{13}C DEPT NMR spectrum (benzene-d_6, 25 °C) of the NMR tube scale reaction of $[U(\kappa^4\text{-}\{(^{tBu2}ArO)_2Me_2\text{-cyclam}\})(NPh)_2]$ (**2**) with of CO_2 (ca. 30 equiv.).

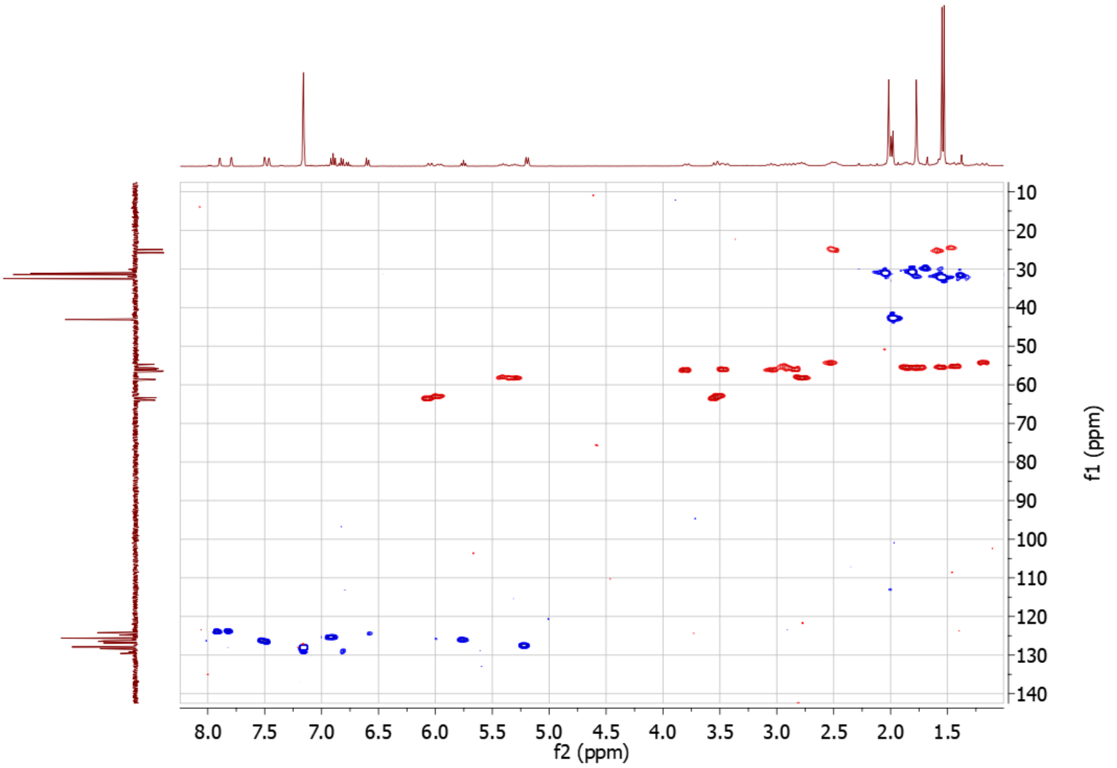

Figure S11. ^{1}H - ^{13}C multiplicity-edited HSQC spectrum (benzene-d_6, 25 °C) of the NMR tube scale reaction of $[\mathrm{U}(\kappa^4\text{-}\{(^{tBu2}\mathrm{ArO})_2\mathrm{Me}_2\text{-cyclam}\})(\mathrm{NPh})_2]$ (**2**) with CO_2 (ca. 30 equiv.) (CH_2 correlations in red; CH_3/CH correlations in blue).

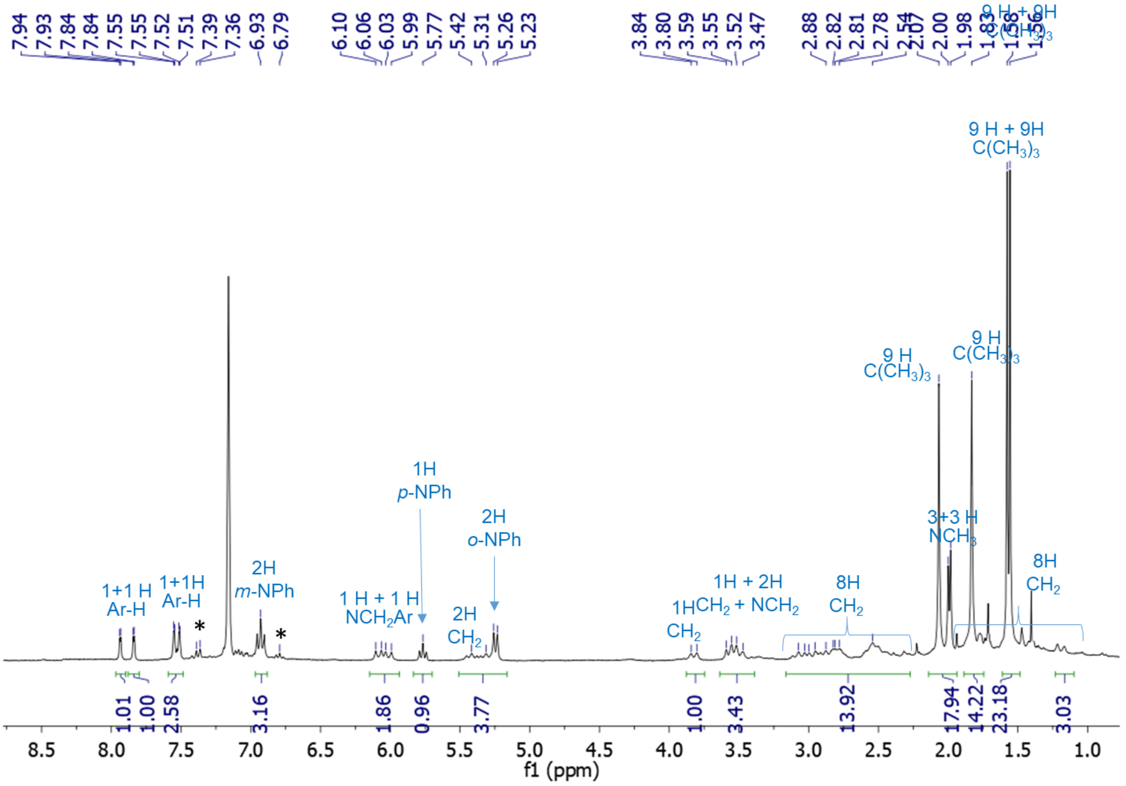

Figure S12. ^{1}H NMR spectrum of a recrystallized sample of $[\mathrm{U}(\kappa^4\text{-}\{(^{tBu2}\mathrm{ArO})_2\mathrm{Me}_2\text{-cyclam}\})(\mathrm{NPh})(\mathrm{O})]$ (**4**) (benzene-d_6, 25 °C). The assignment of the overlapping macrocycle CH_2 protons was based on the ^{1}H-^{13}C NMR experiment (*some contamination resulted from dimerization of phenyl isocyante).

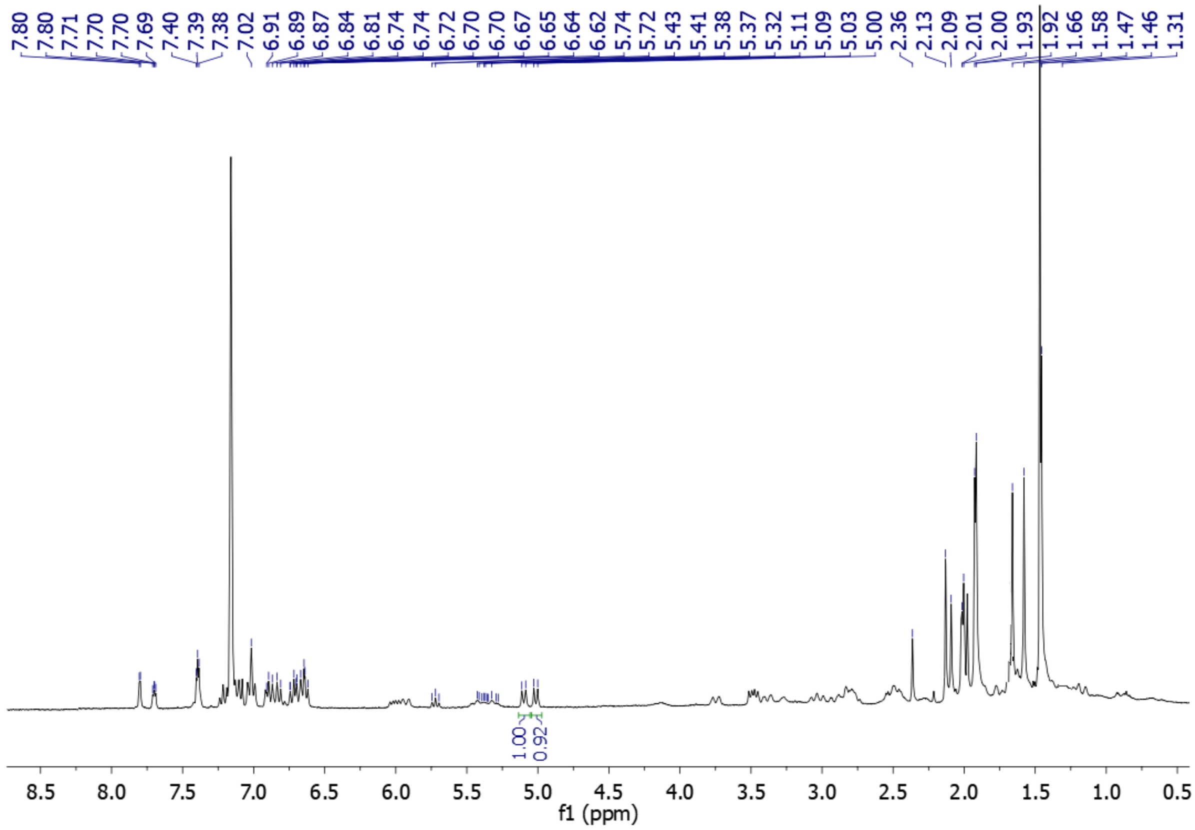

Figure S13. ^{1}H NMR spectrum (benzene-d_6, 25 °C) of the NMR tube scale reaction of [U(κ^4-{(^{tBu2}ArO)$_2$Me$_2$-cyclam})(NPh)(NTol)] (**3**) with of CO_2 (ca. 30 equiv.).

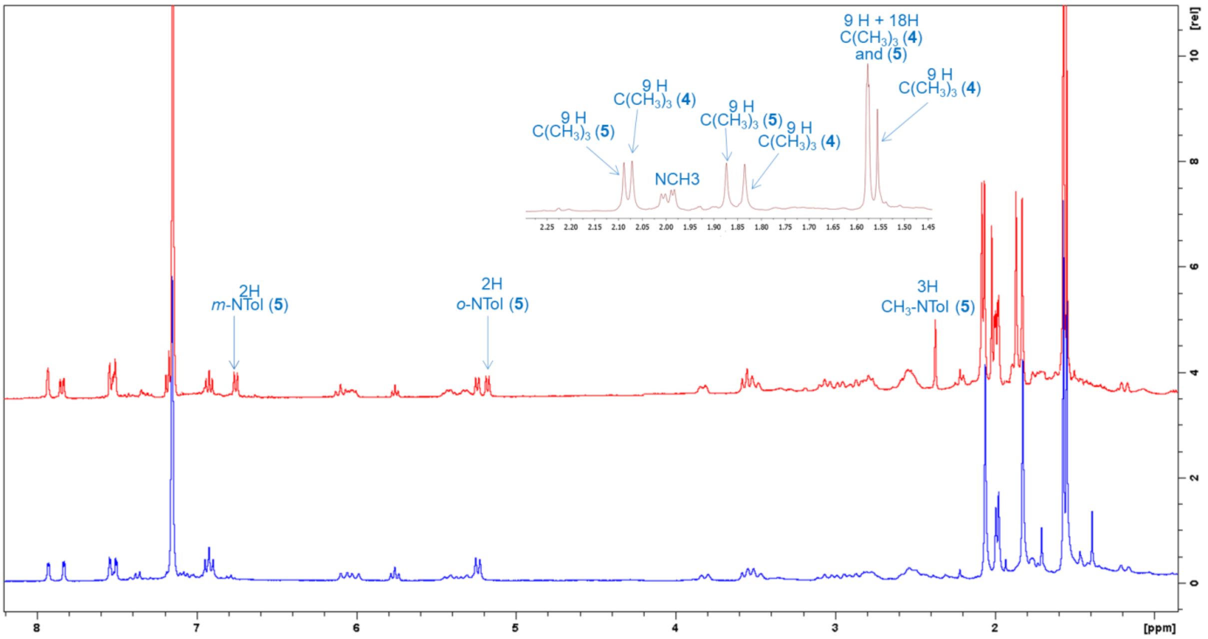

Figure S14. ^{1}H NMR spectrum (benzene-d_6, 25 °C) of (a) NMR tube scale reaction of [U(κ^4-{(^{tBu2}ArO)$_2$Me$_2$-cyclam})(=NPh)(=NTol)] (**3**) with excess of CO_2 after removing the volatiles; (b) [U(κ^4-{(^{tBu2}ArO)$_2$Me$_2$-cyclam})(=NPh)(O) (**4**)].

6. Computational details

The Amsterdam Density Functional[8] (ADF) Program suite version 2017.103 was employed for all the calculations presented in the current paper. The revised Perdew, Burke and Ernzerhof[9, 10] generalized gradient approximate functional was employed in conjunction with Grimme's third generation dispersion[11] corrections (rev-PBE-D3) and the Becke-Johnson[12] mid-range dispersion damping technique. The ZORA[13, 14] quasi-relativistic (scalar) Hamiltonian was employed to account for relativistic effects.

A composite (relativistic) Slater type basis set (bs1) was employed for the several atoms: For uranium a triple zeta type polarized basis set (with a frozen core up to the $4f^{14}$ shell); for oxygen, nitrogen and carbon a double zeta polarised basis set with a $1s^2$ frozen shell; for hydrogen a single zeta basis set.

Geometries were optimised in vacuo with no symmetry restrictions and an analytic Hessian was computed for all intervening species. The reaction coordinate was followed for every transition state for which only one imaginary vibrational mode was found.

For a better energy evaluation a single point run was carried out for every structure replacing the basis set of the lighter elements (C,N,O,H) with a doubly polarised triple zeta basis set (TZ2P) using the same frozen cores. Truhlar's[15, 16] SM12 dielectric continuum solvation scheme was employed at this stage with the appropriate parameters for benzene. These improved potential energy values were used to estimate the free energy in benzene solution by adding the positive terms from the previously calculated gas phase free energies. The entropic corrections of Martin, Hay and Pratt[17] were employed whenever a change in the number of components of a reaction takes place such as in steps A, E, F and J.

A data set collection of computational results is available in the ioChem-BD repository[18] and can be accessed via https://doi.org/10.19061/iochem-bd-6-21.

6. ^{1}H NMR kinetic studies

Samples of **2** in benzene-*d₆* (0.048 M) in a J-Young NMR tube were exposed to an excess of CO_2 (ca. 30 equiv., ~10 atm) at -196.15 °C. The samples were allowed to warm to room temperature (ca. 20 °C) and were immediately transferred to the NMR spectrometer with the probe maintained at the corresponding temperature of the kinetic study. ^{1}H NMR was used to follow the reaction and the spectra were recorded for the following temperatures: 25 °C, 35°C and 45 °C. The duration of the pulse program was taken into account to obtain an accurate time value for the evolution of reagent (**2**) and product (**4**). The resonances of one of the aryloxide protons of [U(κ^4-{(^{tBu2}ArO)$_2$Me$_2$-cyclam})(NPh)$_2$] (**2**) (7.62-7.69 ppm) and of [U(κ^4-{(^{tBu2}ArO)$_2$Me$_2$-cyclam})(NPh)(O)] (**4**) (7.80-7.85 ppm) were integrated and converted to the molar fraction of **2**. As the reaction was performed with a large excess of CO_2, the kinetics was considered to be of pseudo-first-order. A plot of the ln(molar fraction) as a function of time led to the pseudo-first-order rates for each temperature (Figs. S15-S17). From the Arrhenius equation, a plot ln(k_{obs}) versus 1/T (Fig. S18) yielded the value of E_a for the reaction of **2** with CO_2.

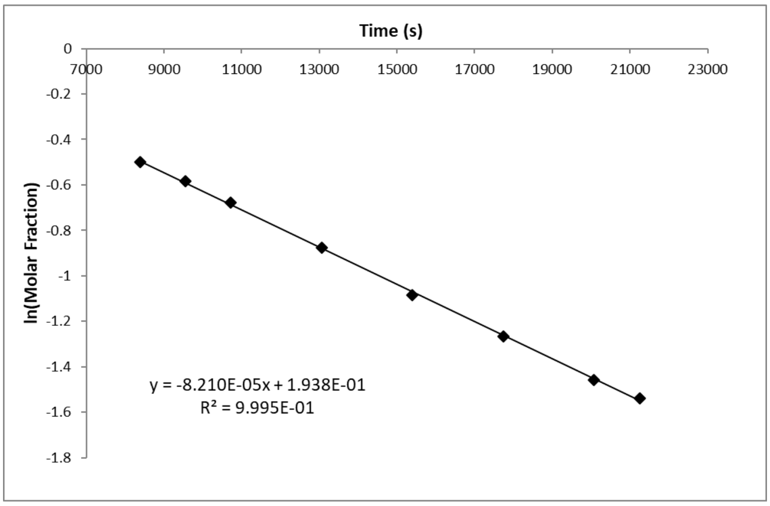

Figure S15: Plot ln(molar fraction) vs time for the reaction of [U(κ^4-{(^{tBu2}ArO)$_2$Me$_2$-cyclam})(=NPh)$_2$] (**2**) with CO_2 at 25 °C.

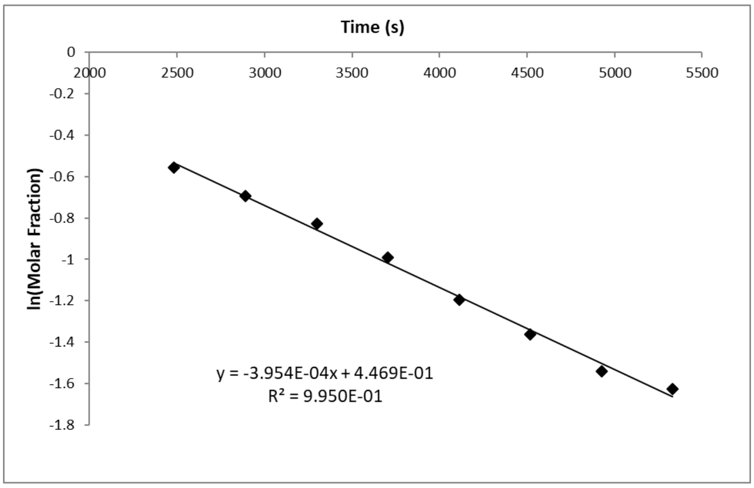

Figure S16: Plot ln(molar fraction) vs time for the reaction of [U(κ^4-{(^{tBu2}ArO)$_2$Me$_2$-cyclam})(=NPh)$_2$]

(**2**) with CO_2 at 35 °C.

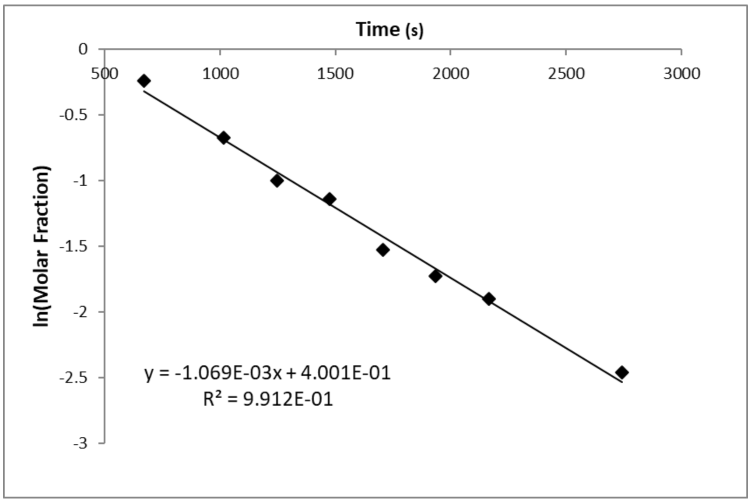

Figure S17: Plot ln(molar fraction) vs time for the reaction of [U(κ^4-{(^{tBu2}ArO)$_2$Me$_2$-cyclam})(=NPh)$_2$] (**2**) with CO_2 at 45 °C.

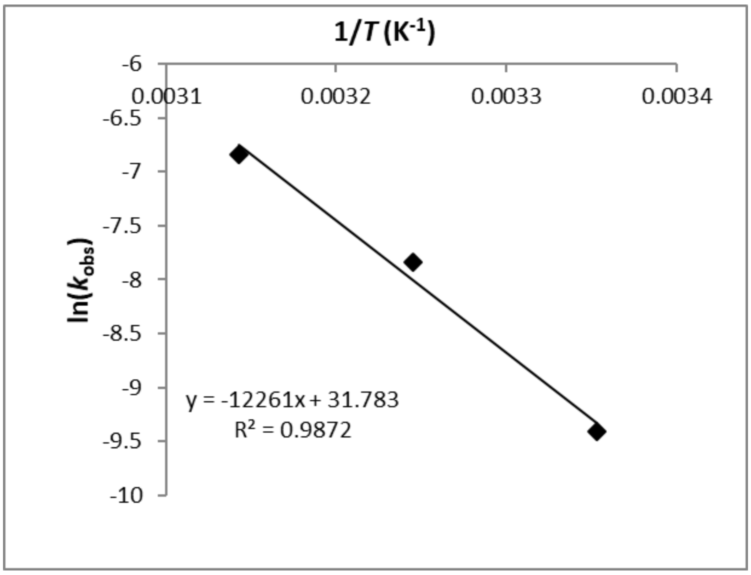

Figure S18. Plot ln(k_{obs}) vs 1/T for the reaction of [U(κ^4-{(^{tBu2}ArO)$_2$Me$_2$-cyclam})(=NPh)$_2$] (**2**) with CO_2. From the Arrhenius equation, ln k = -E_a/RT + lnA, E_a = 102 ± 12 kJ mol^{-1}.

7. References

1. L. Maria, I. C. Santos, V. R. Sousa and J. Marçalo, *Inorg. Chem.*, 2015, **54**, 9115-9126.
2. A. R. Katritzky, T.-B. Huang and M. V. Voronkov, *J. Org. Chem.*, 2001, **66**, 1043-1045.
3. W. Bruker SMART and SAINT; Bruker AXS Inc.: Madison, USA, 2008.
4. G. M. S. B. A. I. M. Sheldrick, Wisconsin, USA, 2004.
5. G. Sheldrick, *Acta Cryst. Section A*, 2008, **64**, 112-122.
6. G. Sheldrick, *Acta Cryst.*, 2015, C**71**, 3-8.
7. L. Farrugia, *J. Appl. Cryst.*, 2012, **45**, 849-854.
8. T. Z. E. J. Baerends, A.J. Atkins, J. Autschbach, D. Bashford, A. Bérces, F.M. Bickelhaupt, C. Bo, P.M. Boerrigter, L. Cavallo, D.P. Chong, D.V. Chulhai, L. Deng, R.M. Dickson, J.M. Dieterich, D.E. Ellis, M. van Faassen, L. Fan, T.H. Fischer, C. Fonseca Guerra, M. Franchini, A. Ghysels, A. Giammona, S.J.A. van Gisbergen, A.W. Götz, J.A. Groeneveld, O.V. Gritsenko, M. Grüning, S. Gusarov, F.E. Harris, P. van den Hoek, C.R. Jacob, H. Jacobsen, L. Jensen, J.W. Kaminski, G. van Kessel, F. Kootstra, A. Kovalenko, M.V. Krykunov, E. van Lenthe, D.A. McCormack, A. Michalak, M. Mitoraj, S.M. Morton, J. Neugebauer, V.P. Nicu, L. Noodleman, V.P. Osinga, S. Patchkovskii, M. Pavanello, C.A. Peeples, P.H.T. Philipsen, D. Post, C.C. Pye, W. Ravenek, J.I. Rodríguez, P. Ros, R. Rüger, P.R.T. Schipper, H. van Schoot, G. Schreckenbach, J.S. Seldenthuis, M. Seth, J.G. Snijders, M. Solà, M. Swart, D. Swerhone, G. te Velde, P. Vernooijs, L. Versluis, L. Visscher, O. Visser, F. Wang, T.A. Wesolowski, E.M. van Wezenbeek, G. Wiesenekker, S.K. Wolff, T.K. Woo, A.L. Yakovlev, http://www.scm.com, *Scientific Computing and Modelling* ADF-2017.
9. Y. Zhang and W. Yang, *Phys. Rev. Lett.*, 1998, **80**, 890-890.
10. J. P. Perdew, K. Burke and M. Ernzerhof, *Phys. Rev. Lett.*, 1996, **77**, 3865-3868.
11. L. Goerigk, H. Kruse and S. Grimme, *ChemPhysChem*, 2011, **12**, 3421-3433.
12. A. D. Becke and E. R. Johnson, *J. Chem. Phys.*, 2005, **123**, 154101.
13. E. van Lenthe, E. J. Baerends and J. G. Snijders, *J. Chem. Phys.*, 1993, **99**, 4597-4610.
14. E. van Lenthe, A. E. Ehlers and E. J. Baerends, *J. Chem. Phys.*, 1999, **110**, 8943-8953.
15. A. V. Marenich, C. J. Cramer and D. G. Truhlar, *J. Chem. Theory Comput.*, 2013, **9**, 609-620.
16. C. A. Peeples and G. Schreckenbach, *J. Chem. Theory Comput.*, 2016, **12**, 4033-4041.
17. R. L. Martin, P. J. Hay and L. R. Pratt, *J. Phys. Chem. A*, 1998, **102**, 3565-3573.
18. M. Álvarez-Moreno, C. de Graaf, N. López, F. Maseras, J. M. Poblet and C. Bo, *J. Chem. Inf. Model.*, 2015, **55**, 95-103.